

LaRuSi₂: a monoclinic variant of the orthorhombic CeNiSi₂-type structure

R. Welter, G. Venturini and B. Malaman

Laboratoire de Chimie du Solide Minéral, Associé au CNRS No 158, Université de Nancy I, B.P. 239, 54506, Vandoeuvre les Nancy Cedex (France)

(Received November 26, 1991)

Abstract

The structure of LaRuSi₂ has been determined and refined from single-crystal X-ray diffraction ($R=0.048$ for ten variable parameters and 157 structure factors). The space group is $P2_1/m$ ($Z=2$). The cell parameters are $a=4.506(5)$ Å; $b=4.110(5)$ Å; $c=8.374(8)$ Å; $\beta=99.45(4)^\circ$. This new type is a distorted variant of the CeNiSi₂-type structure. The cell parameters of the isotypic compound CeRuSi₂ are given.

1. Introduction

In recent papers [1, 2], we have shown the interesting magnetic properties of R(Mn,Fe)Si₂ compounds (R=La–Nd) which crystallize in the TbFeSi₂-type structure. In order to find new isotypic compounds and owing to the similar crystal chemistry of Ru(Os) and Mn(Fe) ternary alloys, we have investigated the R–Ru–Si (R=rare earth) systems. In a preliminary X-ray analysis of LaRuSi₂ alloys powder patterns were observed which seem to belong neither to the TbFeSi₂ [3] nor to the CeNiSi₂ [4] type of structure and led us to study this new phase.

2. Experimental details and results

2.1. Sample preparation and preliminary results

RRuSi₂ compounds (R≡La,Ce) were prepared from stoichiometric amounts of rare earth (purity, 99.9%), ruthenium (purity, 99.99%) and silicon (purity, 99.999), melted in an induction furnace under an argon atmosphere. Ingots were sealed under argon in quartz tubes and were annealed at 1173 K for 5 days. Their purity and their formula were checked by X-ray and microprobe analysis.

Crystallized samples were obtained by melting and slow cooling ingots of LaRuSi₂. A monocrystalline splinter was found after several breakings of a twinned crystal. Preliminary studies were performed on a Weissenberg camera (Cu K α). A monoclinic unit cell was found with the following condition limiting possible reflections: $0k0$ with $k=2n$. This leads to two possible

space groups: $P2_1/m$ and $P2_1$. Cell parameters were obtained by least-squares refinements by curved detector (INEL CPS 120, Co $K\alpha$ powder patterns): $a = 4.506(5)$ Å, $b = 4.110(5)$ Å, $c = 8.374(8)$ Å, $\beta = 99.45(10)^\circ$.

For the isotypic compound $CeRuSi_2$, we obtained $a = 4.478(4)$ Å, $b = 4.085(5)$ Å, $c = 8.303(9)$ Å, $\beta = 102.57(6)^\circ$.

2.2. Structure of $LaRuSi_2$

2.2.1. Structure refinement

Data collection was performed on a Nonius CAD4 automatic diffractometer at the Service Commun de Diffractométrie de l'Université de Nancy I. The conditions for the collection of the single-crystal data and the refinement of the structure are given in Table 1. Absorption has been neglected ($\mu_r < 0.2$). Atomic scattering factors for neutral atoms and anomalous dispersion corrections were taken from ref. 5. All computer programs used were taken from ref. 6. A list of the structure factors can be obtained from the authors on request.

The cell parameter transformations $a' = a$, $b' = 2c + a$, $c' = b$ led to a new unit cell (with the non-standard space group $C1121/m$), similar to those

TABLE 1

Summary of data collection and structure refinement

Molar mass (g)	296.15
Average crystal diameter (μm)	20 approx.
Symmetry	Monoclinic
a (Å)	4.506(5)
b (Å)	4.110(5)
c (Å)	8.374(8)
β (deg)	99.45(10)
V (Å ³)	151.37
Z	2
ρ_{cal} (g cm ⁻³)	6.50
Space group	$P2_1/m$
Radiation	Ag $K\alpha$ (1500 W)
Monochromator	Graphite
Scan mode	$\theta-2\theta$
Take off (deg)	2.5
Record limits	$\theta < 25^\circ$
Linear absorption coefficient μ (cm ⁻¹)	194
Number of intensities	
Recorded	383
Unique and non-zero	335
Kept ($\sigma(I)/I < 0.30$)	157
F (000)	258
Number of parameters	10
Final R value	0.048
Final R_w value	0.051
W	0.4486/
	$[\sigma^2(F_0) + g(F_0)^2]$
g	0.00436

TABLE 2

Lattice parameters of CeNiSi₂, TbFeSi₂ and LaRuSi₂

Compound	<i>a</i> (Å)	<i>b</i> (Å)	<i>c</i> (Å)	γ/β (deg)	Space group
CeNiSi ₂	4.141	16.418	4.068	—	<i>Cmcm</i>
TbFeSi ₂	4.107	16.308	3.933	—	<i>Cmcm</i>
LaRuSi ₂	4.506	16.614	4.110	96.07	" <i>C112₁/m</i> "
LaRuSi ₂	4.506	4.110	8.374	99.45	<i>P2₁/m</i>

TABLE 3

Atomic coordinates of LaRuSi₂^a

Atom	Position	Symmetry	<i>x</i>	<i>y</i>	<i>z</i>
La	2(e)	M	0.0898(5)	1/4	0.2016(2)
Ru	2(e)	M	0.3801(8)	1/4	0.6113(3)
Si(1)	2(e)	M	0.4565(22)	1/4	0.9085(12)
Si(2)	2(e)	M	0.8216(22)	1/4	0.5068(11)

^aSpace group, *P2₁/m*; *B_c* = 0.16(9).

of CeNiSi₂ and TbFeSi₂ (Table 2). Under these conditions, using the atomic coordinates derived from orthorhombic CeNiSi₂ structure as starting point, preliminary refinements in the space group *P2₁/m* led to a reliability factor $R=0.056$. Owing to the lack of information due to the small size of the crystal, only the general temperature factor has been refined yielding the final residual factor $R=0.048$ ($R_w=0.051$). The atomic coordinates and interatomic distances are listed in Tables 3 and 4. The structure is shown in Fig. 1(a).

3. Discussion

In spite of the similarity of their cell parameters the LaRuSi₂ and CeNiSi₂ structures are rather different. First, we have to note the abnormally large value of the a'/c' ratio (1.096) compared with the usual values a/c in CeNiSi₂ compounds (1.038 for LaCu_{0.82}Ge₂ to 0.999 for LaPdGe₂ [7]).

Other discrepancies are related to the atomic positions. For comparison, Table 5 gives the atomic coordinates of CeNiSi₂ (*Cmcm*) and LaRuSi₂ in the non-standard monoclinic description (*C112₁/m*, *i.e.* $x' = z/2 - x$, $y' = z/2$, $z' = y$). It shows that x'_{Ru} and x'_{Si_2} strongly deviate from zero.

LaRuSi₂, CeNiSi₂ and TbFeSi₂ structures are presented in Fig. 1 where the stacking of BaAl₄ and AlB₂ slabs, emphasized by Bodak and Gladyshevskii [4] and Parthé and Chabot [8] in their description of the CeNiSi₂-type structure, are outlined. The examination of the atomic coordinates and structure

TABLE 4

Interatomic distances and angles in the Ru[Si]₄ tetrahedron

Atom 1	Atom 2	Distance (Å)	Atoms	Angle
La	Si(2)	3.055(12)	Si(2)–Ru–Si(2)	97.1(3)°
	2Si(2)	3.150(8)	Si(2)–Ru–Si(2)	119.9(4)°
	2Si(1)	3.174(9)	Si(2)–Ru–Si(1)	116.0(4)°
	2Si(1)	3.185(8)	Si(2)–Ru–Si(2)	112.4(3)°
	Si(1)	3.243(13)		
	2Ru	3.280(7)		
	Si(1)	3.335(14)		
	Ru	3.396(8)		
	2Ru	3.550(6)		
Ru	Si(2)	2.341(12)		
	2Si(2)	2.374(5)		
	Si(1)	2.437(11)		
	Si(2)	2.478(11)		
	2Ru	3.121(6)		
	2La	3.280(7)		
	1La	3.396(8)		
	2La	3.550(6)		
Si(1)	Ru	2.437(11)		
	2Si(1)	2.542(12)		
	2La	3.174(9)		
	2La	3.185(8)		
	La	3.243(13)		
	La	3.335(14)		
Si(2)	Ru	2.341(11)		
	2Ru	2.374(5)		
	Ru	2.478(11)		
	2Si(2)	2.627(13)		
	La	3.055(12)		
	La	3.150(8)		
	2Si(2)	3.534(17)		

drawings shows that the inner part of the BaAl₄ blocks is mainly affected by the monoclinic distortion. This implies two main features, as follows.

(1) Owing to their shift in the [Si]₅ square pyramid, the ruthenium atoms are surrounded by four silicon nearest neighbours with Si–Ru–Si angles to close to 109° (Table 4). If we leave the fifth silicon atom out of consideration, this coordination is close to the Fe(Mn)[Si]₄ tetrahedron encountered in TbFeSi₂ compounds. Correspondingly, this shift leads to a “zigzag” chain of Ru atoms with Ru–Ru distances (3.12 Å) much shorter than the Ni–Ni distances in CeNiSi₂ (3.62 Å) and comparable with the Ru–Ru distances (2.98 Å) observed in LaRu₂Si₂ [9] where the Ru atoms are located in tetrahedra.

(2) The shift of the silicon atoms in their [Ru]₄ tetrahedra leads to the formation of two types of Si(2)–Si(2) distance. One is relatively short ($d = 2.63$ Å) and comparable with the Si(1)–Si(1) separation ($d = 2.54$ Å); the other

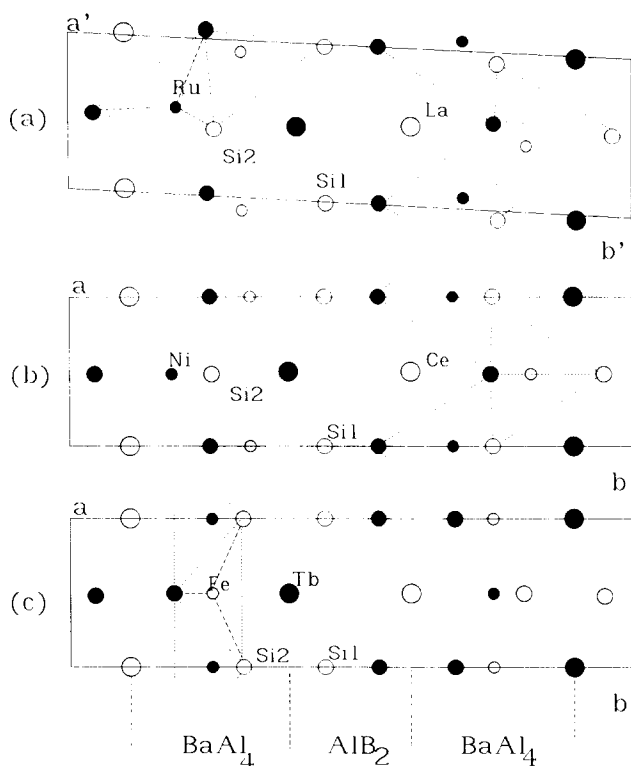


Fig. 1. (a) LaRuSi_2 (in the non-standard group $C1121/m$; see text), (b) CeNiSi_2 and (c) TbFeSi_2 (projection along $[001]$): \circ , $z=1/4$; \bullet , $z=3/4$; ---, TSi_4 tetrahedra and TSi_5 pyramids.

TABLE 5

Comparison of the atomic coordinates of CeNiSi_2 ($Cmcm$) and LaRuSi_2 ($C112_1/m$)^a

Atom	x	y	z	Atom	x'	y'	z'
Ce	0	0.1070	1/4	La	0.0110	0.1008	1/4
Ni	0	0.3158	1/4	Ru	0.9255	0.3056	1/4
Si(1)	0	0.4566	1/4	Si(1)	0.9977	0.4542	1/4
Si(2)	0	0.7492	1/4	Si(2)	0.9318	0.7534	1/4

^aSee text.

($d=3.53 \text{ \AA}$) is much larger than the corresponding distance in CeNiSi_2 ($d=2.90 \text{ \AA}$).

It is rather difficult to explain which of these features is responsible for the structural distortion from CeNiSi_2 to LaRuSi_2 . Nevertheless, our previous studies either on rare earth ruthenium germanides with CeNiSi_2 -type structure [7] or on quaternary rare earth platinum ruthenium germanides with CaBe_2Ge_2 -type structure [10] have shown the poor affinity of ruthenium for the pyramidal

coordination. The occurrence of the LaRuSi₂-type structure, intermediate between those of CeNiSi₂ and TbFeSi₂, probably arises from this fact.

References

- 1 B. Malaman, G. Venturini, L. Pontonnier and D. Fruchart, *J. Magn. Magn. Mater.*, **86** (1990) 347.
- 2 B. Malaman, G. Venturini, J. P. Sanchez and D. Fruchart, *Phys. Rev. B*, **41**(7) (1990) 4700.
- 3 V. I. Yarovets and Yu. K. Gorelenko, *Vestn. L'vovsk. Univ., Ser. Khim.*, **23** (1981) 20.
- 4 O. I. Bodak and E. I. Gladyshevskii, *Sov. Phys. - Crystallogr.*, **14** (1970) 859.
- 5 J. A. Ibers and W. C. Hamilton (eds.), *International Tables for X-Ray Crystallography*, Vol. 4, Kynoch, Birmingham, 1974.
- 6 G. M. Sheldrick, *Shelx 76 - Program for Crystal Structure Determination*, Cambridge University, Cambridge, 1976.
- 7 M. Francois, G. Venturini, B. Malaman and B. Roques, *J. Less-Common Met.*, **160** (1990) 197.
- 8 E. Parthé and B. Chabot, in K. A. Gschneidner, Jr., and L. Eyring (eds.), *Handbook on the Physics and Chemistry of Rare Earth*, Vol. 6, North-Holland, Amsterdam, 1984.
- 9 K. Hiebl, C. Horvath, P. Rogl and M. G. Sienko, *J. Magn. Magn. Mater.*, **37** (1983) 287.
- 10 G. Venturini, B. Malaman and B. Roques, *J. Solid State Chem.*, **79** (1989) 126.